Microstructure observation and quantification of the liquid fraction of M2 steel grade in the semi-solid state, combining confocal laser scanning microscopy and X-ray microtomography

G.C. Gu [a,*], R. Pesci [b], L. Langlois [a], E. Becker [a], R. Bigot [a], M.X. Guo [c]

[a] *Laboratoire de Conception Fabrication Commande (LCFC - EA 4495), Arts et Métiers ParisTech CER Metz, 4 rue Augustin Fresnel, 57078 Metz Cedex 3, France*

[b] *Laboratoire d'Etude des Microstructures et de Mécanique des Matériaux (LEM3), UMR CNRS 7239, Arts et Métiers ParisTech CER Metz, 4 rue Augustin Fresnel, 57078 Metz Cedex 3, France*

[c] *Department of Metallurgy and Materials Engineering (MTM), Catholic University of Leuven, Kasteelpark Arenberg 44, 3001 Leuven, Belgium*

Abstract

Microstructure is of crucial importance to the flow behavior of semi-solid slurries during the thixoforging process. Therefore, a thorough understanding of the microstructure evolution is required. In order to achieve this, high temperature confocal laser scanning microscopy (CLSM) and high energy X-ray microtomography were used to investigate the microstructure evolution of several steel grades (M2, 100Cr6 and C38LTT) during the heating process from as-received conditions to the semi-solid state. It was found that the microstructure development of M2 can be directly studied at high temperature via these two techniques. Two types of small carbides (MC and M_6C) were present in the as-received state, while totally new interconnected carbides of specific size and composition were formed from liquid zones after cooling. It was also noted using CLSM that the diffusion rate of the alloying elements during the cooling of M2 was very low. This confirms that the volume fraction of the liquid phase of M2 at high temperature can be evaluated by three-dimensional X-ray microtomography in situ at high temperature and on quenched specimens. Contrary to M2, the microstructure of the steel grades 100Cr6 and C38LTT in the semi-solid state can only be revealed by CLSM at high temperature. All these observations are discussed in terms of microstructural development and liquid fraction during heating.

Keywords: M2 steel grade; Semi-solid; Liquid fraction; CLSM; X-ray microtomography

1. Introduction

Thixoforging, an innovative technology, is recognized as a near-net-shaping process which takes advantage of the thixotropic properties of semi-solid slurries to produce complex parts with good mechanical properties, usually in a one-step operation. The nondendritic microstructure, which consists of spheroidal grains in a liquid matrix, plays an important part in successful thixoforging, because it determines the thixotropic properties of metallic materials in the semi-solid state [1]. Therefore, it is necessary to have a thorough understanding of the microstructure evolution during semi-solid processing. In partially liquid metallic alloys, the volume fraction of solid phase and its distribution (solid skeleton) are of great importance in the thixoforging process, because they crucially influence the rheological behavior [2] and therefore the flow behavior of a material during its formation [3]. Normally, the microstructure of materials in the semi-solid state is always characterized by means of quenching experiments from the partial liquid state. However, the microstructure characterization by

* Corresponding author. Tel.: +33 03 87 37 54 30; fax: +33 03 87 37 54 70.

E-mail addresses: guochao.gu@gmail.com (G.C. Gu), raphael.pesci@ensam.eu (R. Pesci).

quantitative metallography on quenched samples, especially steel grades, is very difficult due to the high diffusion rate of elements and phase transformation behavior during quenching [4]. Moreover, considering random sections, two-dimensional (2-D) image analyses may not give a representative image of the structure and can sometimes lead to invalid conclusions, in particular for the characterization of the liquid phase networks and the steric arrangement of the solid phase in the semi-solid state. Thus, three-dimensional (3-D) analyses can be preferable for microstructure characterization, especially if they are carried out in situ, directly at high temperatures.

In situ techniques are increasingly used and developed to study the microstructure evolution. Some 2-D in situ techniques have been employed for the real-time observation of microstructure evolution during melting and solidification. Iqbal et al. [5] used synchrotron X-ray diffraction to observe grain nucleation and growth in situ during solidification of aluminum alloys. Attallah et al. [6] investigated the initiation of incipient melting of primary γ' in an Ni-base superalloy by using high temperature confocal laser scanning microscopy (HT-CLSM). Compared to the 2-D in situ techniques, high energy X-ray microtomography, which is a non-destructive technique, offers the possibility to retrieve 3-D information from a given specimen. It can be used to characterize the morphology of materials and to obtain some quantitative results in the semi-solid in three dimensions through ex situ and in situ investigations [7]. This technique has been successfully used to investigate the overall and local microstructural changes occurring during partial remelting of aluminum alloys directly at high temperature [8], because the solid and liquid phases present good absorption contrast thanks to the large difference in chemical compositions. Such in situ observations have never been performed on steel grades in the semi-solid state; only ex situ investigations on M2 steel grade have been carried out on quenched specimens from the semi-solid state [9].

The thixoforging of alloys with low melting points, such as aluminum and magnesium alloys, has been industrialized [4,10]. However, steel thixoforging is still at the research stage. Because of some advantages of steel thixoforging, such as a low forging force, the possibility to form complex parts and to reduce forming operations, and final parts with high mechanical properties, interest in the commercialization of this process is on the rise. Considering the industrial applications and suitability of the thixoforging process, C38LTT (low temperature for thixoforging) [11] 100Cr6 [12] and M2 [13], were investigated using CLSM and X-ray microtomography. The aim of this paper is to present a detailed experimental study of the microstructure evolution of these three steel grades prior to the thixoforging process using both in situ and ex situ technologies. The volume fraction of liquid will be focused on as it is the most influential parameter of thixoformability. The instrumental device and the experimental procedure are described and the microstructure evolution is analyzed. In addition, the 3-D microstructure of a complex M2 steel billet in the semi-solid state is reconstructed and discussed.

2. Experimental procedure

2.1. Materials

Three different steel grades were used in this study: hypo-eutectoid steel C38LTT, hypereutectoid steel 100Cr6 and M2 high speed tool steel. C38LTT was manufactured by ASCOMETAL steel producer specifically for the thixoforming process. 100Cr6 is a commonly used steel and also has good thixoformability. M2 steel was produced by hot rolling at a temperature of ~1100 °C; after quenching, it was then annealed three times for 1 h at 540 °C. Thanks to its high content in alloying elements, especially tungsten and molybdenum, which have a high difference in X-ray absorption compared to iron, M2 was investigated in the semi-solid state as a "model" to predict the behavior of the other two grades, which are more industrially used. The chemical composition of these three steel grades is given in Table 1.

2.2. HT-CLSM

A LasertecTM 1LM21H-SVF17SP CLSM was used to make some in situ investigations of the microstructure evolution directly during heating to the semi-solid state and during cooling to room temperature. It was combined with a heating stage mounted at the focal point of an ellipsoidal gold-plated infrared image furnace, powered by a 1.5 kW 100 V halogen lamp (Fig. 1a and b).

Small samples 5 mm in diameter and 3 mm in height were used for the in situ observations at high temperature. Each specimen was sectioned, ground and mechanically polished down to 1 μm. For the experiments, each specimen was placed in an alumina crucible positioned on a Pt stage in the furnace below a quartz viewing window. During heating, a high purity argon atmosphere was charged and titanium foils were placed near the specimens in order to avoid the oxidation phenomenon. Different steel samples were heated following the heating cycles shown in Fig. 1c. They were heated at a low heating rate until a plateau was reached at ~300 °C. After 50 s of isothermal holding, the samples were heated at a heating rate of 200 °C min^{-1} to the predetermined temperature. Due to the nature of the temperature measuring and controlling system (Fig. 1a), there is a difference in temperature between the real and measured temperatures during rapid heating. A thermal calibration showed that the temperature difference between the specimen surface and the recorded thermocouple temperature did not exceed ±15 °C. The specimen's surface was initially etched in order to reveal the microstructure and adjust the focus and the magnification of the CLSM. After each thermal cycle, the specimens were prepared a second time for microstructure characterization at room temperature, after cooling, by grinding, polishing and Nital 2% etching.

Table 1
Chemical composition of the steel grades.

	Chemical composition (wt 10^{-3}%)																	
	C	Si	Mn	S	P	Ni	Cr	Mo	Cu	Al	Sn	As	B*	V	Ti	Nb	Ca*	N*	W
C3SLTT	399	596	1424	83	77	91	130	29	114	3	9	9	4	89	15	0	10		0
100Cr6	988	230	326	6	7	210	1428	82	194	31	13	10	2	4	3	1	2	109	0
M2	850	35	250	⩽40	⩽40	200	4100	5000	100					1900					6400

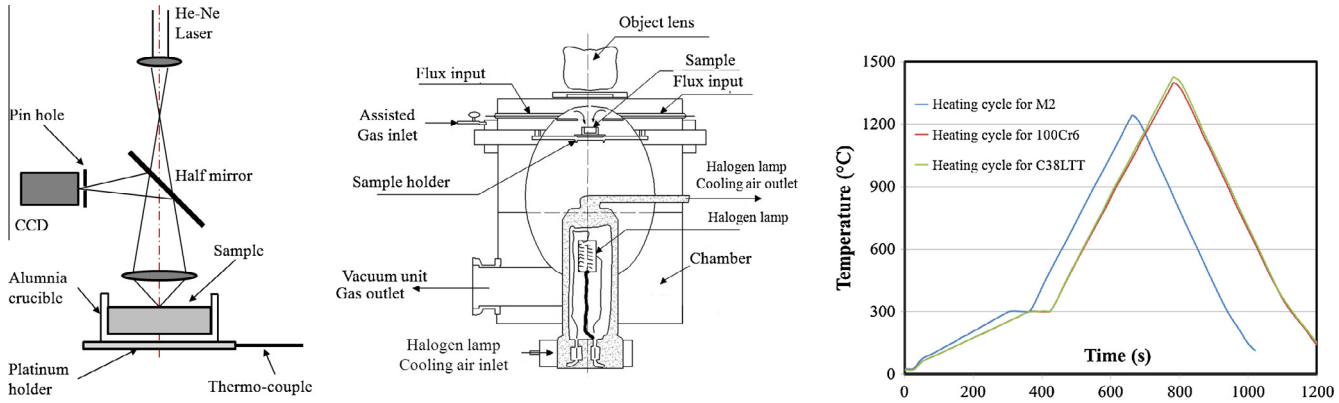

(a) Schematic view of HT-CLSM without infrared image furnace.

(b) Schematic view of CSLM heating system

(c) The actual thermal cycles performed in the HT-CLSM

Fig. 1. Schematic view of CLSM with infrared image furnace (a and b) [14]. The thermal cycles performed in the CLSM for various steel grades are shown in (c).

They were finally observed with both optical and scanning electron microscopes.

2.3. High energy X-ray microtomography

Both in situ and ex situ X-ray microtomography experiments were carried out on the high-energy ID15A beamline at the ESRF (European Synchrotron Radiation Facility) in Grenoble, France. The samples 1.2 mm in diameter and 30 mm in height were electrodischarge-machined from rolled steel bars. During the tests, each sample was mounted on translation and rotation stages in order to achieve a good alignment with the X-ray beam before the measurement and a 360° rotation for 3-D observations. An induction heating system developed in our laboratory at ENSAM was used to heat the specimens to the semi-solid state for in situ observations. The X-ray beams went through the specimen while the specimen was continuously rotating over 360°. The incident X-ray beam was directed onto the rotating samples with a constant energy of 60 keV. The transmitted beam was recorded using a fast DALSTAR Pantera 1M60 CCD detector with a ~25 ms exposure time. In full frame mode (1024 × 1024 pixels), the scan time for a total rotation was ~20 s. The transmitted information was digitally transcribed into a grey level proportional to the number of transmitted photons. During in situ tests, the induction heating rate was very fast. No protective gas was used during heating, due to the strong thermal exchange between the protective gas and the sample. In order to avoid significant microstructure changes in one X-ray scan, the same specimen was tested at various temperatures (in both the solid state and semi-solid state). It was assumed that the microstructure changes at a constant temperature were not significant in one tomographic scan. The effective pixel size was ~1.2 μm and 3600 projections were captured. Fig. 2 shows a schematic view of 3-D X-ray microtomography. The induction heating system was only used for the in situ observations; ex situ experiments were performed on parts quenched from the semi-solid state. The X-ray microtomographic slices were then reconstructed and the different volumes obtained were processed and analyzed with the image analysis software ImageJ.

2.4. Ex situ experiments: induction heating

Thanks to its high heating speed, repeatability and ability to heat in a protective atmosphere, the induction heating approach is preferably used for industrial thixoforging applications. In order to study the microstructure development and liquid phase distribution in the billet, an M2 steel

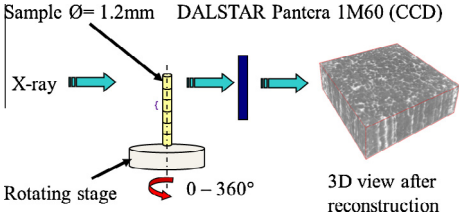

Fig. 2. Schematic diagram of X-ray tomography set-up.

billet 38 mm in diameter was partially heated to the semi-solid state using a one-step heating route. Due to thermal exchanges and penetration effects, a bell-shape temperature distribution was expected: the temperature decreased with decreasing radius and height, and the material at the bottom remained in the solid state due to the lack of heat source in this area (Fig. 3). As a consequence, the volume fraction of liquid throughout the billet must be very different, because of the heterogeneous temperature distribution in the billet. A pyrometer was used to control the heating process by measuring the temperature at point C; when it reached ~1300 °C, the billet was directly water-quenched without any holding time to freeze the microstructure presented in the semi-solid state. Then, some cylindrical samples (Ø1.2 mm) were taken in various directions (electrodischarge machining), as shown in Fig. 3.

2.5. Metallography and image analysis

Microstructure observations and analyses were also conducted at room temperature with an optical microscope and a JEOL 7001FLV scanning electron microscope (SEM). The distribution of different alloying elements was finally investigated using an EDS system from Oxford Instruments. All samples observed in two dimensions were etched using 2% Nital (2 ml HNO_3 + 98 ml ethanol).

3. Results and discussion

3.1. Materials in as-received state

Optical and SEM micrographs of the three steel grades (C38LTT, 100Cr6 and M2) in the as-received state are shown in Fig. 4. First, C38LTT is a ferritic pearlitic steel in the as-received state (Fig. 4a) with the presence of MnS and TiCN inclusions (Fig. 4a) and the grain size is ~10 μm; 100Cr6 steel shows only a pearlitic microstructure with an average grain size of ~10 μm, Fig. 4c. Then, the results showed that M2 steel (average grain size ~10 μm) contained large amounts of carbides (Fig. 4d) which was confirmed by EDS analyses shown in Fig. 5: the whiter particles are M_6C type carbides, rich in tungsten and molybdenum, while the darker ones are MC-type carbides, rich in vanadium, tungsten and molybdenum. Moreover, the presence of microsegregation bands parallel to the working direction in the longitudinal direction (Fig. 4e) confirms the manufacturing process.

3.2. In situ observations with CLSM

The in situ observations were first performed on C38LTT and 100Cr6 in order to study the microstructure evolution and the liquid distribution in particular, via partial remelting from the as-received state. M2 steel grade was then investigated.

Fig. 6 presents the snapshots taken at different temperatures on C38LTT in the attempted thermal cycles shown in Fig. 1. The sample was etched before in situ observations, which leads to a rugged surface; since CLSM is sensitive to the relief, as a result, the grain boundaries could be observed as shown in Fig. 6a. A solid–solid transformation occurred at ~740 °C (Fig. 6b); it was characterized by a total change of the brightness of the image. Given the temperature, this phase transformation must have been austenization. Ferrite and pearlite were transformed into austenite in white in Fig. 6b. However, some MnS inclusions were still remaining in the matrix and along the grain boundaries after austenization, as shown in Fig. 6c–e. With increasing temperature, the austenite grain boundaries were revealed by thermal etching, and the liquid films were first observed along the grain boundaries (Fig. 6d). However, when comparing Fig. 6d and e, it was found that the liquid content increased a lot during a very short time. Moreover, the liquid distribution at the surface of the sample was not uniform. During cooling, after liquid/solid and solid/solid phase transformations, the microstructure mainly consisted of ferrite, pearlite and MnS inclusions (Fig. 6g). After in situ observations, the samples were etched with Nital 2%. The microstructures before and after etching could be compared in Fig. 6h and i. Ferrite in

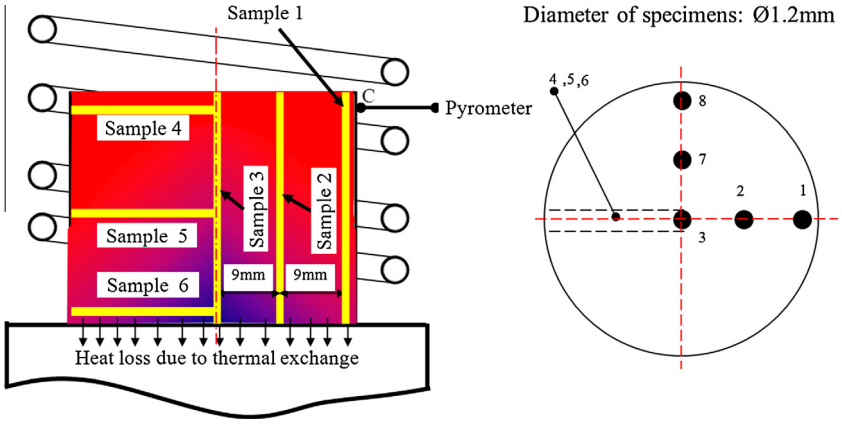

Fig. 3. Schematic of the set-up for partial melting experiments and the position of the samples.

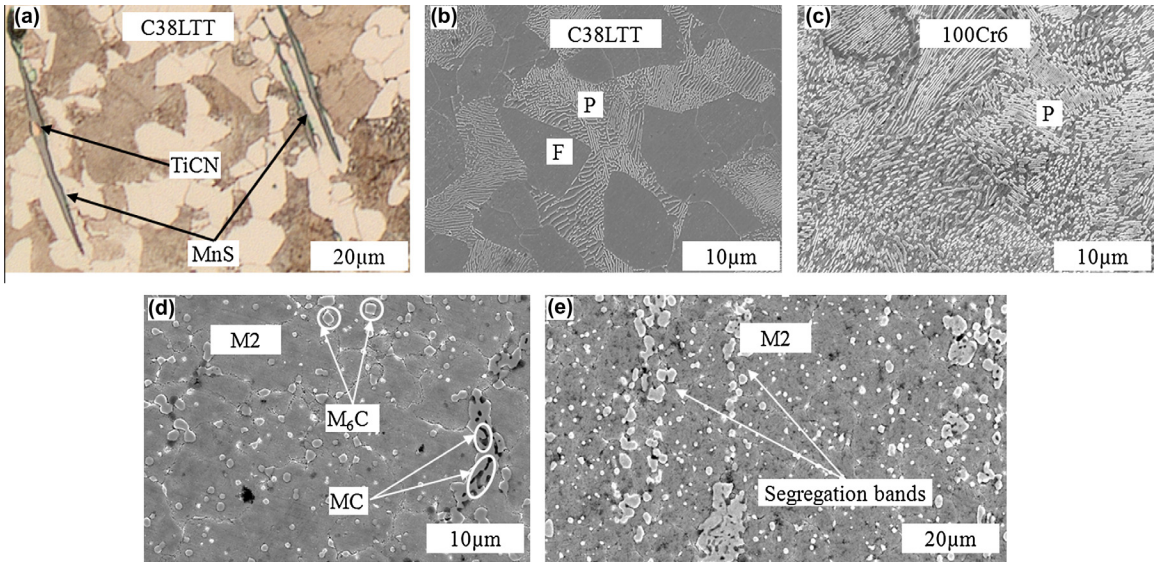

Fig. 4. Micrographs of as-received samples. C38LTT in (a) longitudinal direction (optical) and (b) transversal direction (SEM); 100Cr6 in (c) transversal direction; M2 in (d) transversal direction (SEM) and (e) longitudinal direction (SEM). P: pearlite; F: ferrite.

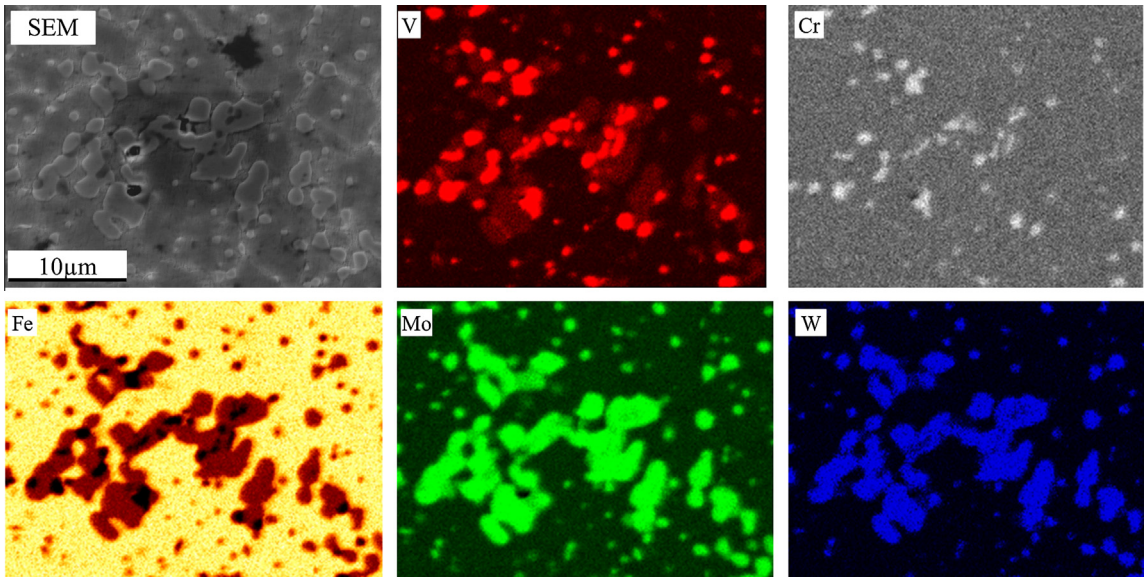

Fig. 5. SEM–EDS mapping of as-received M2 steel.

white, pearlite in grey and MnS inclusions in black were observed in Fig. 6i. The liquid films shown in Fig. 6h mainly correspond to the ferrite at the grain boundaries shown in Fig. 6i. However, the former liquid zones cannot be precisely detected from the microstructure cooled from the semi-solid state to room temperature.

The microstructure evolution of 100Cr6 during heating and cooling can be observed in Fig. 7. During heating, the sample surface remained unchanged until ~770 °C (Fig. 7b). Pearlite and the grain boundaries revealed by SEM (Fig. 7a) were not visible with CLSM because of the lack of relief at the surface. During heating the austenization starting temperature was ~770 °C. With increasing temperature, thermal etching revealed the austenite grain boundaries (Fig. 7c); the grains grew with increasing temperature. When temperature exceeded the solidus temperature of 100Cr6 (~1290 °C), the liquid first appeared along the grain boundaries (Fig. 7d) and then in the matrix (Fig. 7e). The liquid film finally recovered the whole surface of the sample (Fig. 7f); with decreasing temperature, it started to solidify and finally transformed into pearlite (Fig. 7g). After the in situ observations, the samples were also investigated post mortem. Fig. 7h and i presents the micrographs of the surface before and after etching, respectively. The oxidation of the sample surface can be observed (Fig. 7h). The boundaries may be related to the grain boundaries, since they are deeper than the surface in the semi-solid state as compared in Fig. 7h and i. After etching,

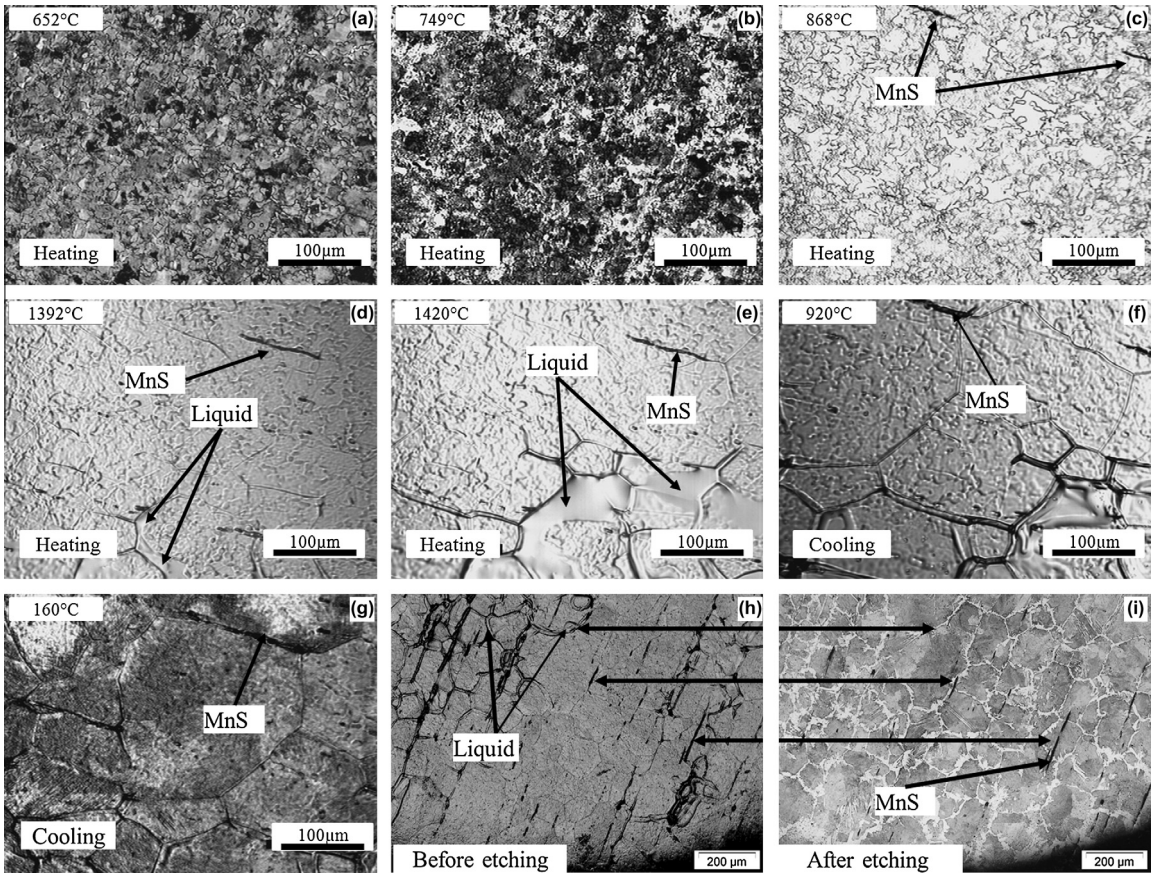

Fig. 6. (a–g) HT-CLSM snapshots for the sequence of partial remelting of C38LTT during heating at 200 °C min^{-1} until 1420 °C and the subsequent cooling. (h) Sample surface after cycle and (i) optical micrograph of the material shown in (h).

pearlite is well observed in the sample, but it is very difficult to find a correlation between the final microstructure at room temperature and that in the semi-solid state. From all the snapshots, it can be found that the liquid fraction on the sample surface increases rapidly in a small temperature range, from 1300 °C to 1350 °C.

From the results of CLSM on these two steel grades (C38LTT and 100Cr6), it could be seen that the semi-solid range was relatively small. Therefore, it will be difficult to control it with a good reproducibility in industrial applications. In addition, after cooling from the semi-solid state, it was very complicated to retrieve the previous microstructure in the semi-solid state. Even when performing some EDS mappings on quenched materials with prolonged exposing time, the former liquid zones could not be determined. Therefore, another steel grade, M2, was introduced in this study, because of its high content in alloying elements which can be easily detected by different techniques.

The specimen surface revealed the evolution of the microstructure of M2 in the solid state at various temperatures (Fig. 8a–c). Before reaching the austenization starting temperature (~830 °C), a microstructure with small grains and isolated carbides could be observed. With increasing temperature, the carbides decreased in size; the different elements diffused into austenite. However, as the content of chemical elements is very high, it was impossible to dissolve all these carbides before melting started (Fig. 8c). When the solidus temperature was reached, the alloying elements diffused into the liquid phase (Fig. 8d) in which the solubility was higher. The liquid appeared mainly along the grain boundaries (Fig. 8e). An interconnected liquid phase was formed with increasing temperature, as shown in Fig. 8e. Since the liquid was rich in alloying elements, it was easy to study the evolution of the liquid phase at high temperature. After cooling, this liquid phase became new carbides with exactly the same size and location (Fig. 8f), even with the low cooling rate available with the CLSM (~200 °C min^{-1}). Besides the liquid/solid transformation, there were some solid/solid phase transformations during cooling (405 °C, Fig. 8h). At room temperature, a microstructure differing from that in the as-received state in grain size, distribution of carbides and morphology was obtained (Fig. 8).The newly formed carbides were surrounding the grains which were bigger than those in the as-received state; few alloying elements remained inside the grains, as shown by EDS analyses.

With this technique, it was therefore possible to investigate the microstructure evolution directly at high temperature, but it was not easy to quantify the liquid fraction mainly because of the magnification and the field of view

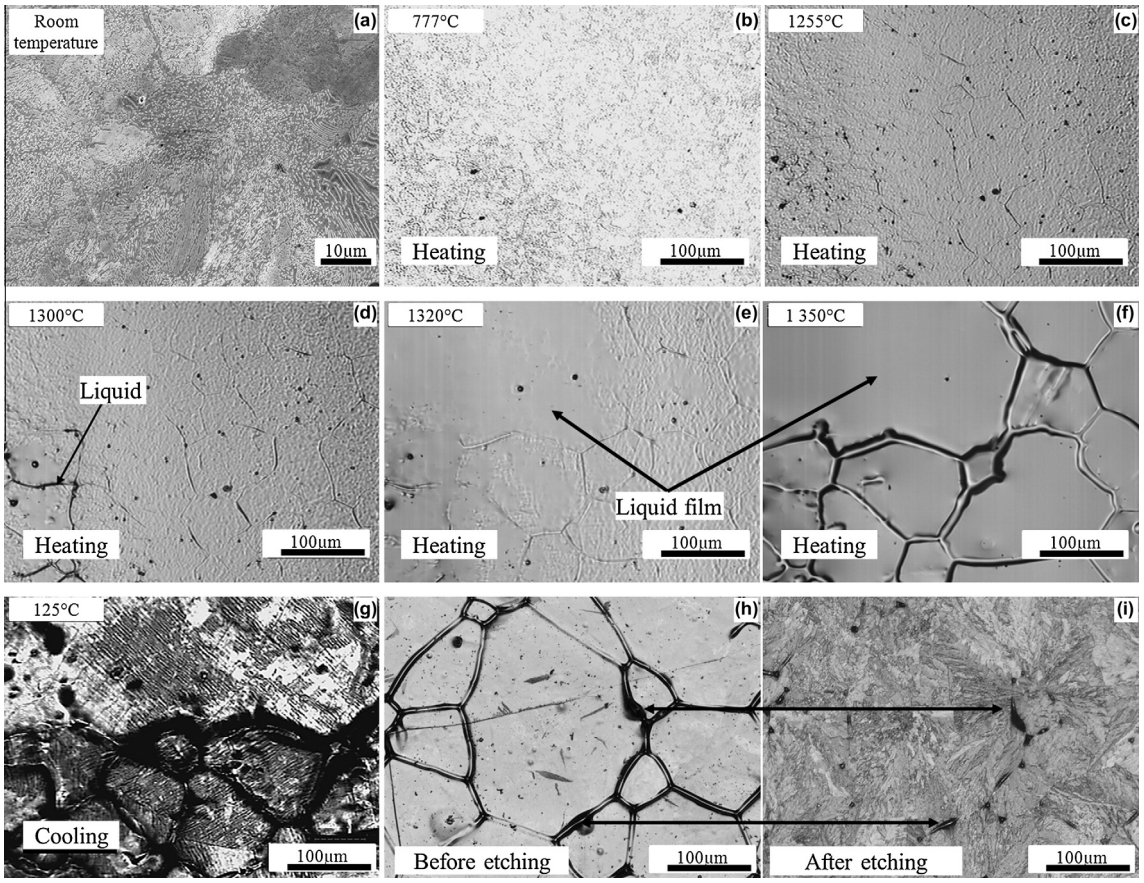

Fig. 7. (a) SEM micrograph of 100Cr6 in the as-received state. (b–g) HT-CLSM snapshots for the sequence of partial remelting of 100Cr6 during heating at 200 °C min^{-1} until 1350 °C and the subsequent cooling. (h) Sample surface after thermal cycle and (i) optical micrograph of the material shown in (h).

available. However, it was found that the freezing range of M2 was relatively large and, more importantly, that the liquid phase in the semi-solid state of M2 could be preserved after cooling and corresponded to newly formed big carbides, even at a low cooling rate. It means that it must be possible to quantify the liquid fraction ex situ by image analyses, especially on the material quenched from the semi-solid state.

According to the CLSM results for these three steel grades, it was possible to investigate the microstructure evolution (solidus temperature, liquid appearance, grain size, etc.), but due to the small field of view, it was difficult to make a liquid fraction evaluation. Since the X-ray microtomography can provide a 3-D microstructure information, some experiments were then performed on these steels.

3.3. X-ray microtomography

3.3.1. In situ observations by high energy X-ray microtomography

Fig. 10 presents some 2-D in situ tomographic slices of C38LTT and M2 samples, numerically extracted in the semi-solid state. Since there is not a big amount of alloying elements in C38LTT and since these elements are not far from iron in the Periodic Table, there is no difference in X-ray absorption (absorption contrast) between the solid and liquid phases. A homogeneous microstructure can be observed for C38LTT as shown in Fig. 10a; similar results were observed for 100Cr6 for the same reasons. On the contrary, for M2, a heterogeneous microstructure can be obtained with different phases visible, as shown in Fig. 10b. The liquid is rich in alloying elements thanks to the high content in alloying elements which are far from iron in the Periodic Table (especially Mo and W); because of the different absorption of alloying elements, the white zones are considered to be liquid zones containing heavy elements while the grey zones correspond to the austenitic matrix. Since the slice is taken from the transversal direction, no segregation bands are observed. This confirms with CLSM that the microstructure evolution of M2 can be studied through in situ X-ray microtomography.

Fig. 11 presents a set of 2-D in situ tomographic slices of the sample numerically extracted in the solid (Fig. 11a) and semi-solid state (Fig. 11b), respectively.

One can clearly observe the evolution of oxidation on the sample skin even at a high heating rate due to the absence of protective gas. Before heating, a small oxide layer caused by electrodischarge machining was observed on the sample skin; with increasing heating, the thickness

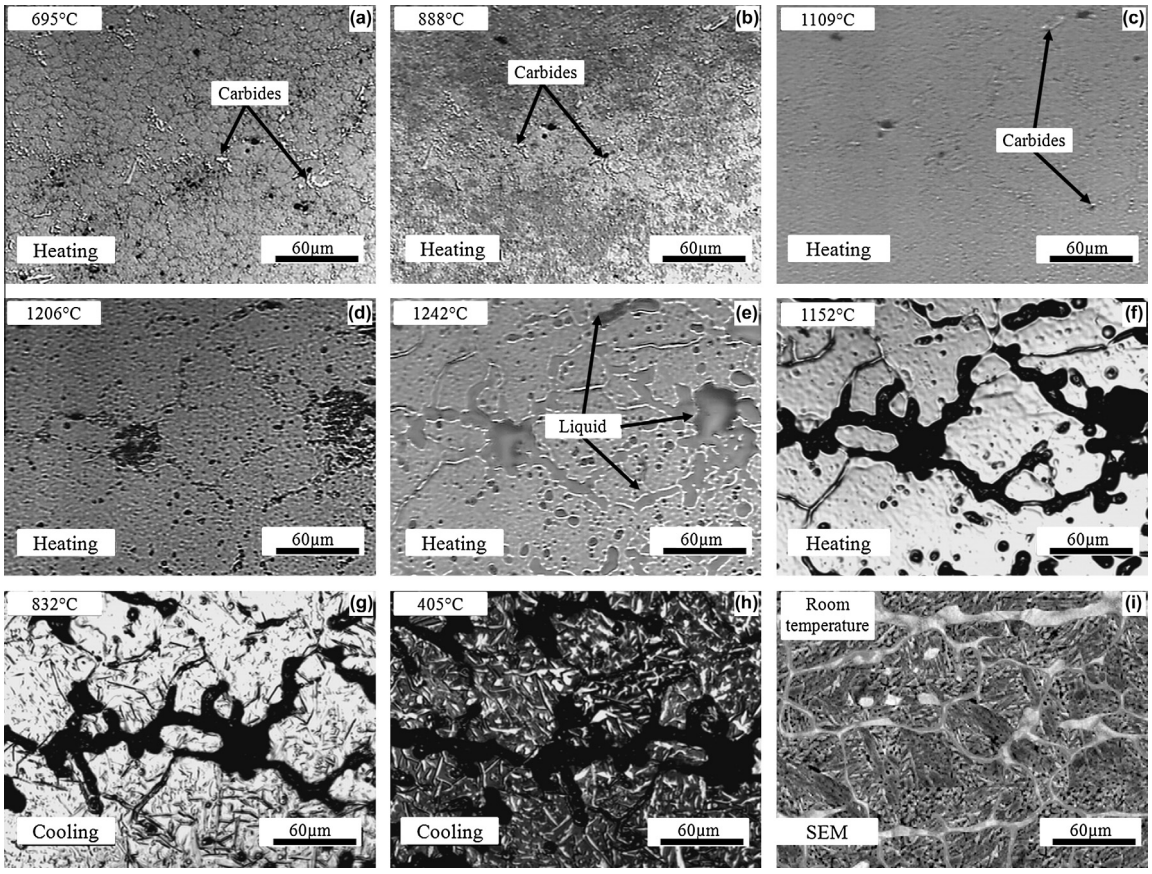

Fig. 8. (a–h) HT-CLSM snapshots for the sequence of partial remelting of M2 during heating at 200 °C min^{-1} until 1250 °C and the subsequent cooling. (i) is a SEM micrograph after cooling from the semi-solid state.

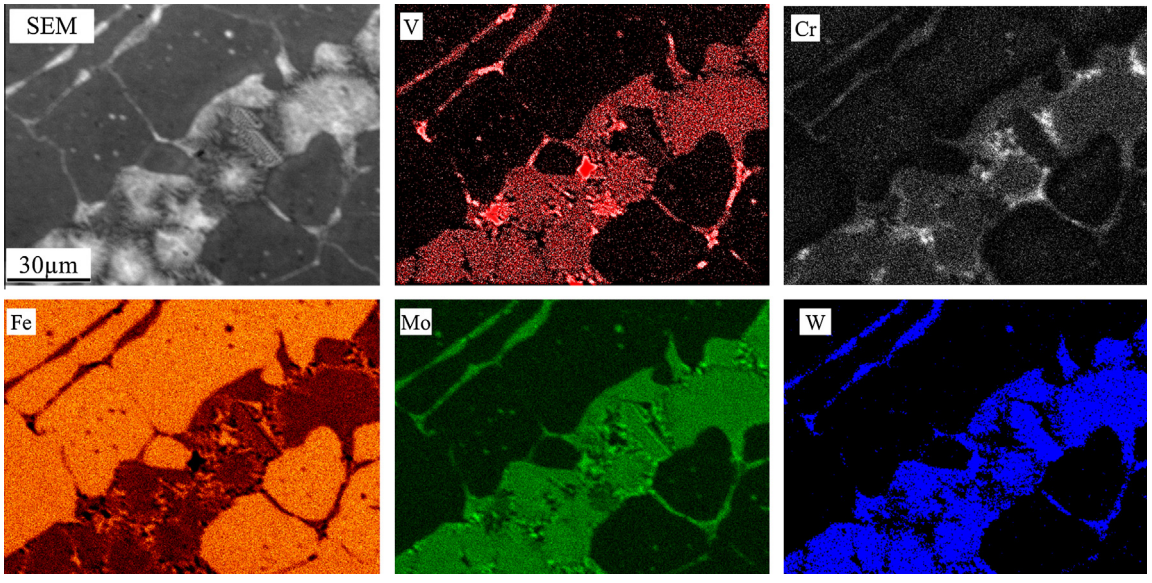

Fig. 9. SEM–EDS mapping of the M2 quenched from the semi-solid state.

of this layer increased significantly, as shown in Fig. 11a–c. The heating time from Fig. 11a–c was less than 1 min. Despite that, what was interesting was that the microstructure development during heating could also be observed. The white zones in the tomography images were liquid because they were rich in alloying elements, especially Mo and W; they were also interconnected. The morphology and distribution of these white zones were similar

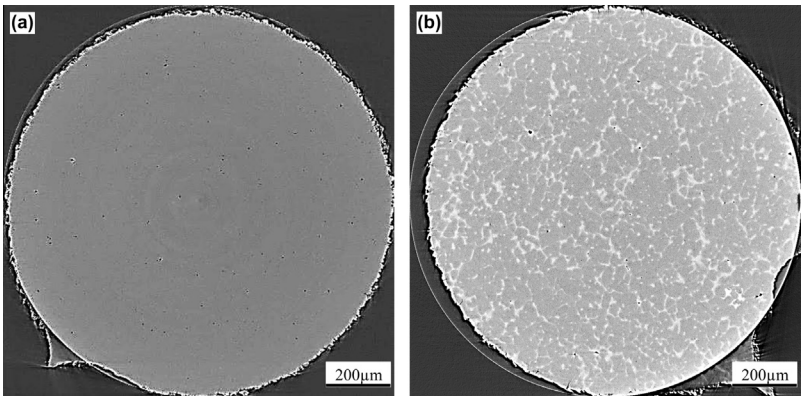

Fig. 10. Tomography slices of C38LTT at ~1410 °C and M2 at ~1300 °C.

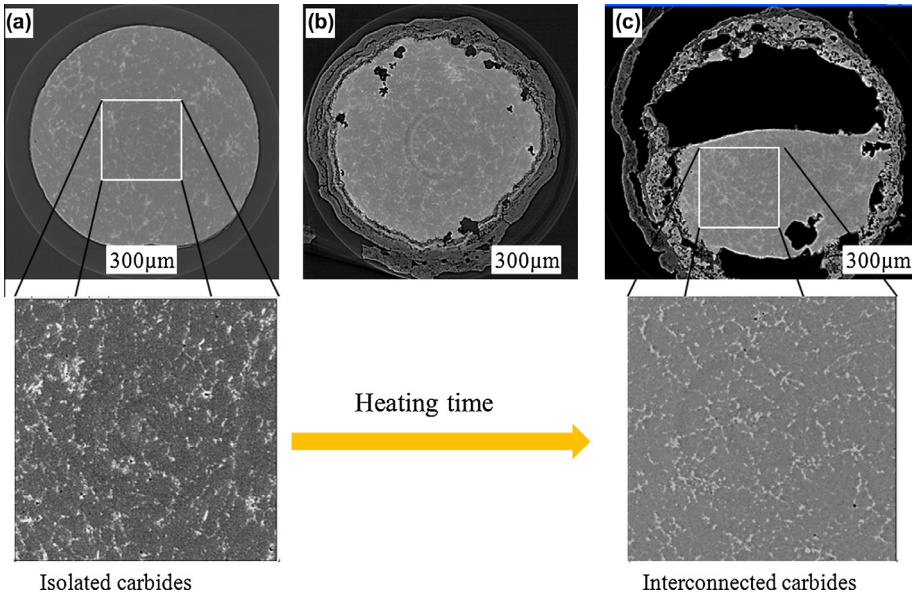

Fig. 11. X-ray microtomography slices showing the microstructure evolution at different heating times.

to those observed in SEM images after quenching, as shown in Fig. 9, corresponding to newly formed carbides as seen with CLSM experiments. Moreover, these new carbides formed after quenching are located at the grain boundaries where the liquid is supposed to appear first at high temperature [15]. A 1.2 µm resolution was used in this study: it was the best achieved so far with this technique. This means that some very small liquid zones/carbides cannot be detected or some assembled carbides are probably considered as one large carbide. However, since the differences of microstructure in the solid state and semi-solid state are significant, it is possible to use X-ray microtomography in order to observe the microstructure evolution in a whole billet heated to the semi-solid state, directly at high temperature or after quenching, and to make a real quantification of the liquid fraction throughout this billet.

3.3.2. Ex situ X-ray microtomography on M2 after quenching

The results of CLSM on M2 have shown that the liquid zones can be preserved by cooling, even at a low cooling rate. It means that after quenching, it must be possible to precisely locate and quantify the liquid fraction obtained at high temperature. As compared to CLSM and SEM, X-ray microtomography provides 3-D information on microstructure, as stated in Ref. [9]. In addition, a larger field of view can improve the precision of the quantification of liquid fraction and reduce the uncertainty. In order to study the real volume liquid fraction at high temperature, ex situ X-ray microtomography experiments were performed on the samples electrodischarged from the partially heated billet in Fig. 3. Three types of microstructure can be observed in different positions depending on the height (or temperature) in the billet. Fig. 12 shows the 3-D stacks of

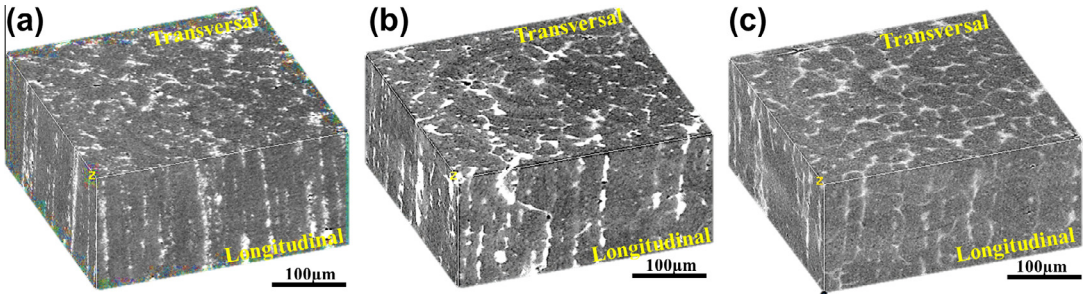

Fig. 12. 3-D stacks of M2 taken from different zones showing various microstructures. (a) 100% solid state. (b) Low liquid fraction. (c) High liquid fraction.

M2 reconstructed at three different positions. Fig. 12a is taken at the bottom of the sample (solid state). Fig 12b and c is taken in the semi-solid state. In Fig. 12a, only very small carbides are present; their size is similar to those in the as-received state. In Fig. 12b, big interconnected carbides coexist with small isolated carbides that are not fully diffused into the liquid phase. Finally, Fig. 12c mainly shows big interconnected carbides mainly located at the grain boundaries where the liquid is supposed to appear in the semi-solid state; these carbides make it easier to define the grain size at high temperature and after quenching. Some segregation bands can also be observed in longitudinal sections along the samples. Similar to the SEM micrographs of the as-received state of M2, the isolated carbides are shown in transversal sections in Fig. 12a. By image analysis, the volume fraction of white zones can be quantified; it varies from ~11% to ~22% with increasing height from bottom to top.

After the total reconstruction of X-ray tomography slices taken from the partially melted and water-quenched billet, it was found that the microstructure at various positions is different. For better legibility, only typical reconstructed stacks at different zones are given. Table 2 shows their fraction of carbides while Table 3 presents their 3-D microstructure. Due to the effect of penetration depth during induction heating and thermal exchange, the temperature distribution throughout the slug is heterogeneous: the temperature increases with height and radius. Depending on temperature in the part, there are mainly three zones which show different microstructures. Considering sample 1 as an example, in the height interval of 0–11 mm (Table 3 (05) and (06)), the microstructure is similar to that in the

Table 2
Fraction of carbides evaluated by 3-D tomography in different positions.

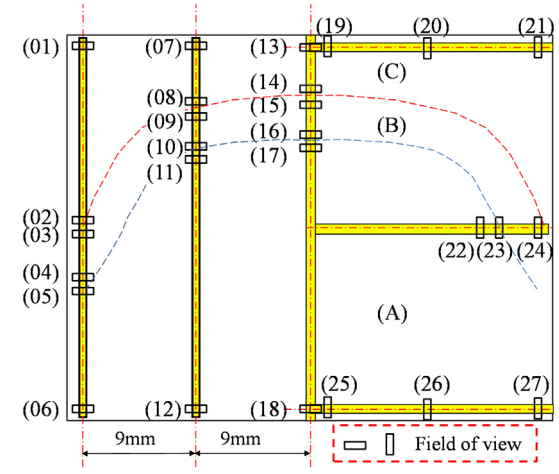

Sample	Position		Fraction of carbides Fc (%)
	H(mm)	R(mm)	
(1)	29	18	21.1±1.2
(2)	16	18	15.2±0.5
(3)	15	18	14.9±1.4
(4)	12	18	11.9±0.4
(5)	11	18	10.3±0.7
(6)	1	18	11.1±0.8
(7)	29	9	17.4±0.8
(8)	25	9	13.9±0.7
(9)	24	9	13.2±0.8
(10)	22	9	10.9±0.7
(11)	21	9	10±0.4
(12)	1	9	11.5±0.6
(13)	29	0	14.8±0.5
(14)	26	0	13.6±0.2
(15)	25	0	12.6±0.8
(16)	23	0	10.7±0.5
(17)	22	0	10.5±0.3
(18)	1	0	11.1±1.1
(19)	29	0.6	15.0±0.7
(20)	29	9	17.0±0.4
(21)	29	18	20.9±1
(22)	15	11	11.7±0. 8
(23)	15	13	13±0.6
(24)	15	18	14.2±0.4
(25)	1	0.6	10.6±0.6
(26)	1	9	10.8±0.7
(27)	1	18	11.4±0.5

Fc and Fl are the volume fraction of carbides and liquid, respectively.

Table 3
3-D tomographic stacks reconstructed from the partial remelted and quenched part shown in Table 2.

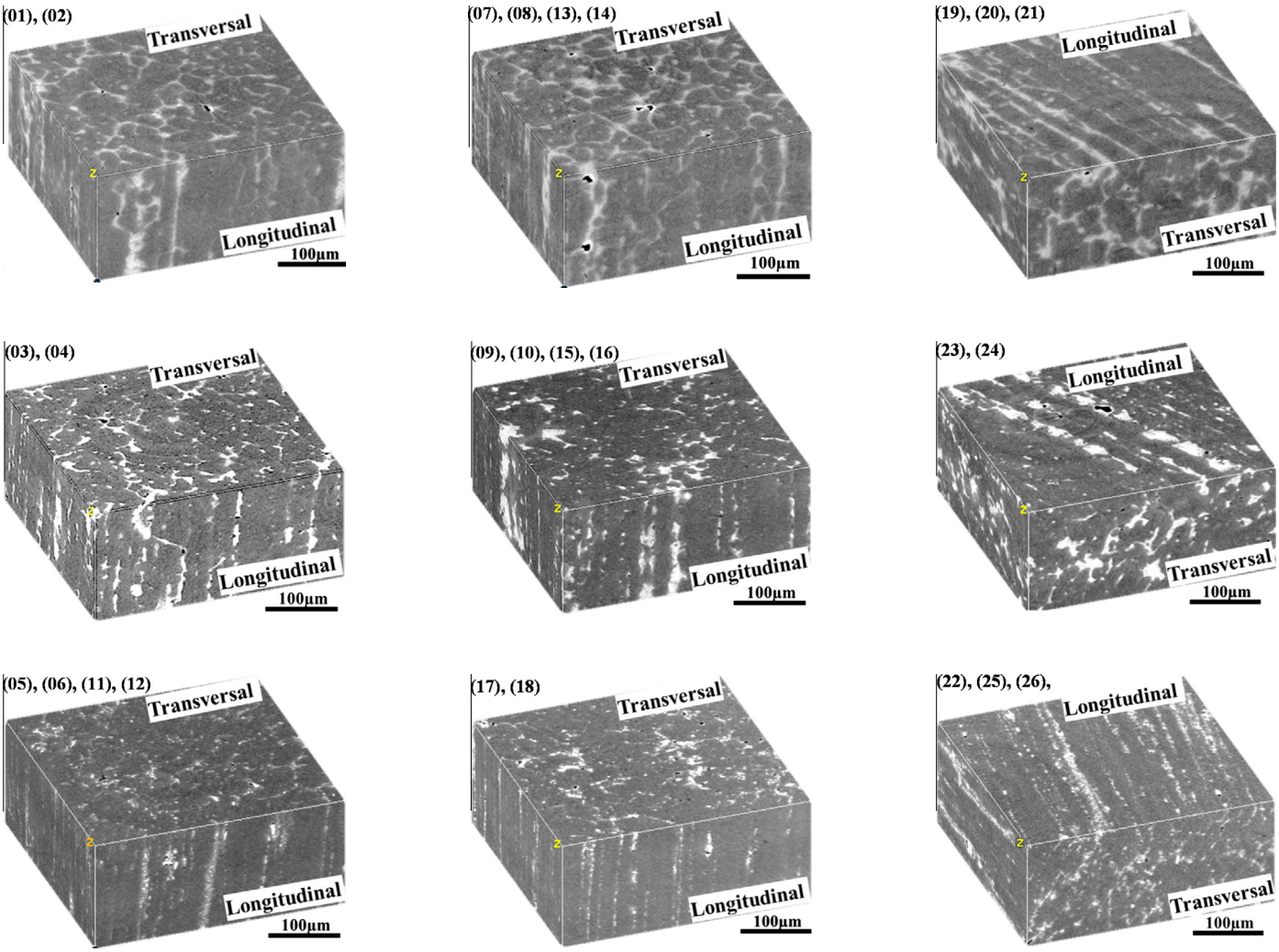

as-received state: isolated small carbides and carbide segregation bands are visible in longitudinal section and the fraction of carbides *Fc* is ~11%. The material in this interval therefore remains in the solid state. Then, with increasing height where the temperature is higher, part of the original carbide particles are dissolved and the alloying elements in carbides start diffusing to the liquid zones where the solubility is higher. During quenching, new carbides are formed from liquid zones. Meanwhile, from the results of CLSM on M2, it could be concluded that few alloying elements diffused into the matrix during quenching. As shown in Table 3 (03) and (04), both big interconnected and isolated small carbides can be observed. By image analysis, the volume fraction of carbides increases from ~11% to ~15% with increasing height from 12 mm to 16 mm. Finally, mainly interconnected big carbides are observed in the 3-D stacks of sample 1 over the height of 16 mm. In these zones, the initial small carbides were fully diffused into the liquid phase due to high temperature. After quenching, the newly formed interconnected carbides are shown in Table 3 (01) and (02). As a conclusion, depending on the morphology of sample 1, there are mainly three zones: Zone A, a solid zone in which the microstructure and the volume fraction of carbides are similar to that of the as-received state; Zone B, a semi-solid zone with still undissolved original carbides and Zone C, a semi-solid zone where the original carbides were totally dissolved into liquid during heating, leading to the apparition of new big carbides after quenching. In Zone C, the carbide fraction is equal to the liquid fraction Fl whereas in Zone B, it is difficult to get the liquid fraction due to the coexistence of the new big carbides formed from previous liquid zones and original carbides. When comparing the evolution of the microstructure and liquid fraction of axial samples (samples 1, 2 and 3), the results are quite similar, but with a certain discrepancy. For example, the height interval of Zone A in sample 2 and sample 3 is

0–22 mm and 0–24 mm, respectively. Zone C in samples 2 and 3 covers the height interval 24–30 mm and 25–30 mm, respectively. The microstructure evolution in the radial samples (samples 4, 5 and 6) is presented in Table 3 (19)–(27). Due to the heterogeneous temperature distribution in the partially remelted billet, the microstructure changes depend on the position. The segregation bands can be observed in all the radial samples but with different morphologies. In sample 4, the liquid zones preferentially develop from the grain boundaries and appear very clear after quenching, which makes obvious the definition of the new grain boundaries. As sample 6 remains in the solid state, the segregation bands mainly contain small carbides instead of interconnected carbide networks, as observed in sample 4. Since the sample 5 is in Zone B, both small isolated carbides and interconnected big carbides networks are observed. If we compare the morphology and the carbide fraction at the same height and radius, but in different zones (e.g. in Tables 2 and 3, (01) vs. (21), (02) vs. (20), (13) vs. (19), (03) vs. (24), (06) vs. (27), (12) vs. (26) and (18) vs. (25)), it can be noted that the induction heating is axisymmetric; the expected bell-shape of temperature distribution is therefore confirmed.

4. Discussion

CLSM was used to investigate the occurrence of the liquid phase in various steel grades via partial melting. The microstructure evolution of the grades during heating was similar, with solid/solid and solid/liquid phase transformations. The first austenization was observed when the temperature reached Ac1, followed by grain growth, the initiation of localized melting with increasing temperature and then, ultimately, more grain boundary wetting. Classically, differential scanning calorimetry/differential thermal analysis and dilatometric experiments were used for determining the phase transformation temperature. Similar to the results observed from CCT curves, the comparison of the austenization starting temperature of the three studied steels based on the CLSM snapshots showed that it was much higher for M2 steel than that of the two other grades, which may have resulted from the alloying elements. In addition, the diffusion rate of alloying elements was much lower than that of carbon, leading to a longer time for total austenization. Moreover, during heating, in each grade, there was a significant grain growth when comparing the grain size in the as-received state and at high temperatures. In general, the austenite grains grow with increasing temperature and time. Moreover, the carbon content in grades also influences the grain growth during heating; The grain growth and diffusion process are thermally activated and related to the liquid fraction, since liquid provides a much faster diffusion path than solid; Manson-Whitton et al. [16] stated that the grain coarsening rate should decrease with increasing liquid fraction because once a continuous liquid path is present around the solid phase, the energy is used for the increasing of liquid instead of grain growth. The LSW (Lifshitz, Slyozov and Wagner) analysis, suggested initially by Greenwood [17] and later developed independently by Lifshitz and Slyozov [18], and Wagner [19], may not be appropriate for estimating the grain size because it is a classical theory for coarsening of a low volume fraction dispersed second phase. The coarsening of semi-solid alloys with a liquid fraction can be better described in terms of the migration of grain boundary liquid films [20] which separate the grains than by considering diffusion fields around isolated solid grains (LSW analysis) [16]. In addition, grain coalescence is also thought to be an important factor for the grain growth, as stated by Tzimas and Zavaliangos [21]. When comparing the grain size of C38LTT and 100Cr6 at high temperature with the same heating rate, it is bigger for 100Cr6 than for C38LTT. In addition, the grain size of M2 steel is much smaller than that of the other two grades due to the pinning ability of the carbides [13]. The grain growth during reheating is important for the thixoforging process. During thixoforging, large grains cannot flow into thin sections as easily as those of a finer size. Furthermore, the mechanical properties of the part will be weakened if the grain size is larger.

During melting of C38LTT and 100Cr6 by CLSM, it can be observed that the liquid distribution on the sample surface is not uniform, as shown in Figs. 5e and 6e. This phenomenon can result from the flatness of the sample surface or the heterogeneity of the material; it may also result from the orientation of the grains. Melting is always initiated at solid surfaces, solid/solid interfaces or at associated defects, since they provide heterogeneous nucleation sites for the liquid phase. In addition, the melting of different crystal surfaces occurs at different temperatures, which has been observed in many experiments [22]. For example, Frenken et al. [23] and Pluis et al. [24] have found that {1 1 0} surface pre-melts below the thermodynamic equilibrium melting point T_0, while the {1 1 1} surface may exhibit non-melting up to and even above T_0 for some metals.

The microstructure of each grade at high temperature is not the most classical one for the thixoforging process – solid spherical grains surrounded by a liquid matrix – but is composed of equiaxed solid grains with connected liquid films. These solid grains can become more spherical with increasing holding time in the semi-solid state, which is good for the thixoforging process. During heating, the carbides dissolved and the alloying elements diffused into the eutectic liquid, which may have penetrated the grain boundaries when the local grain boundary energy (γ_{GB}) was twice as great as the solid/liquid surface energy (γ_{SL}) [25]. Then, melting at the sharp asperities of the equiaxed grains resulted in near-spheroidal grains. However, in industrial conditions, it is always a compromise between the forging time and the forging efficiency. Therefore, the holding time for obtaining more spherical grains is not long in industrial applications. In addition, some steel parts have been thixoforged with such microstructures in the semi-solid state [11,26]. A successful thixoforging process

not only depends on the microstructure in the semi-solid state but also on the liquid fraction and temperature sensitivity. From the results of CLSM, it can be observed that the temperature sensitivity of C38LTT and 100Cr6 is high as compared to that of M2 steel, which brings a difficulty in temperature control during heating. In general, at a liquid fraction lower than 30%, the solid skeleton will support the material's weight and can be handled like a solid. During a deformation, the solid skeleton will be broken and the solid grains can roll or pass over each other while the liquid phase surrounding them acts as a lubricant. Thus, the material might behave in a thixotropic way. However, when the liquid fraction is much lower (<10%), the liquid films in grain boundaries may not be sufficient for grains to flow freely against each other, resulting in an unsuccessful thixoforging process. Tzimas and Zavaliangos [27] have discussed various methods for a precise liquid fraction evaluation. In this study, the X-ray microtomography has been performed on M2 steel for evaluating the real 3-D volume fraction of liquid fraction, directly in the semi-solid state but also after quenching by measuring the volume fraction of carbides. The results are very interesting since it is possible to show the heterogeneity of the volume fraction of liquid in the studied heated billet. As stated in Ref. [15], considering the resolution of different techniques, the good agreement between 2-D image analysis (resolution: 1 nm) and 3-D X-ray microtomography (1.2 μm) for the measurement of the liquid fraction provides an opportunity to quantify the liquid fraction when the microstructure at high temperature can be preserved by quenching. It means that it will then be possible to investigate the liquid fraction and the liquid flow in each zone of complex thixoforged parts made in M2 steel after quenching. The uncertainty of the X-ray microtomographic results comes not only from the image analysis, but also the technique itself. As shown in Table 2, there are three different microstructure zones in the billet. The uncertainty in these three different zones may vary. The newly formed carbides and original carbides coexist in Zone B; it is difficult to distinguish the original carbides from the newly formed carbides by X-ray microtomography. However, they could be identified by SEM with a good resolution. At the same time, from the SEM micrographs, some newly formed small carbides which are different from the original ones in morphology and content could also be observed; they are probably related to the entrapped liquid in the semi-solid state. The entrapped liquid in the semi-solid state is usually observed in extruded or rolled materials, caused by self-blocking remelting. Since it is a 3-D feature, it can only be precisely quantified by 3-D techniques. In this work, some 3-D measurements of entrapped liquid were performed in Zone C, with a volume fraction of ~2.2%. This entrapped liquid phase is well known not to participate in the deformation; thus, it contributes to an increase in the solid fraction. It may not therefore influence the thixoforging process significantly, especially when the entrapped liquid is released by shearing, which breaks the bonds between grains (disagglomeration process).

5. Conclusions

In this work, various techniques have been used to investigate the evolution of the liquid fraction and the microstructure of three different steel grades. The HT-CLSM was first used to observe the microstructure evolution during heating from the solid state to the semi-solid state: solid/solid and solid/liquid transformations, grain growth and initiation of the liquid phase along grain boundaries. Due to the initial microstructure, the chemical composition and the grain size among others, the temperature sensitivity of these steel grades were different. In particular, the liquid fraction on the sample surface increased rapidly in a small temperature range for C38LTT and 100Cr6 steels and it has been shown that the liquid phase of M2 steel at high temperature could be preserved, even at low cooling rate, through newly formed carbides rich in tungsten and molybdenum, which means that some quenching experiments can be used for studying the microstructure at high temperature for this steel. After being induction-heated and water-quenched, the microstructure evolution of a billet of M2 steel was therefore investigated using 3-D X-ray microtomography. After total reconstruction, several zones were identified and discussed, with a precise quantification of the liquid fraction in the semi-solid state. The good agreement with 2-D SEM image analyses proves that the quantification of the liquid fraction is possible for M2 steel. Both image analysis and X-ray microtomography can be used in the future for the investigation of the liquid fraction and the liquid flow on quenched thixoforged parts, for which the microstructure at high temperature is preserved. Since the X-ray microtomography gives access to in situ 3-D morphology of a multiphase sample at high temperature, it will be very interesting to transform data obtained by X-ray microtomography into a finite element representation and to use it to run numerical simulations for investigating the thixoforging process.

Acknowledgements

The authors acknowledge the helpful discussions with Joris Van Dyck at the Catholic University of Leuven and Mr. Scheel at the ESRF. They also warmly thank Marc Wary (Arts et Métiers ParisTech CER Metz) for his technical support and advice.

References

[1] Spencer D, Mehrabian R, Flemings MC. Metall Mater Trans B 1972;3:1925.
[2] Bigot R, Favier V, Rouff C. J Mater Process Technol 2005;160:43.
[3] Becker E, Favier V, Bigot R, Cezard P, Langlois L. J Mater Process Technol 2010;210:1482.
[4] Hirt G, Kopp R. Thixoforming: Semi-solid Metal Processing. Aachen. Wiley-VCH Verlag, KGaA; 2009.

[5] Iqbal N, van Dijk NH, Offerman SE, Moret MP, Katgerman L, Kearley GJ. Acta Mater 2005;53:2875.
[6] Attallah MM, Terasaki H, Moat RJ, Bray SE, Komizo Y, Preuss M. Mater Charact 2011;62:760.
[7] Salvo L, Cloetens P, Maire E, Zabler S, Blandin JJ, Buffière JY, et al. Nucl Instrum Methods Phys Res B 2003;200:273.
[8] Limodin N, Salvo L, Suéry M, DiMichiel M. Acta Mater 2007;55:3177.
[9] Gu GC, Pesci R, Becker E, Langlois L, Bigot R, Scheel M. Acta Mater 2012;60:948.
[10] Kirkwood DH, Suéry M, Kapranos P, Atkinson HV, Young KP. Semi-solid processing of alloys. Berlin: Springer; 2010.
[11] Becker E, Bigot R, Langlois L. Int J Adv Manuf Technol 2009;48:913.
[12] Püttgen W, Hallstedt B, Bleck W, Löffler JF, Uggowitzer PJ. Acta Mater 2007;55:6553.
[13] Omar MZ, Atkinson HV, Howe AA, Palmiere EJ, Kapranos P, Ghazali MJ. J Mater Sci 2009;44:869.
[14] Heulens J, Blanpain B, Moelans N. J Eur Ceram Soc 2011;31:1873.
[15] Gu G, Pesci R, Becker E, Langlois L, Bigot R. Key Eng Mater 2012;554–557:547.
[16] Manson-Whitton ED, Stone IC, Jones JR, Grant PS, Cantor B. Acta Mater 2002;50:2517.
[17] Greenwood GW. Acta Metall 1956;4:253.
[18] Lifshitz IM, Slyozov VV. J Chem Phys Solids 1961;19:35.
[19] Wagner C. Z Electrochem 1961;65:581.
[20] Annavarapu S, Doherty RD. Acta Metall Mater 1995;43:3207.
[21] Tzimas E, Zavaliangos A. Mater Sci Eng A 2000;289:228.
[22] Jin ZH, Lu K. Philos Mag Lett 1998;78:29.
[23] Frenken JWM, Maree PM, Van der veen JF. Phys Rev B 1986;34:7506.
[24] Pluis B, D vd Gon AW, vd Veen JF, Riemersma AJ. Surf Sci 1990;239:265.
[25] Omar MZ, Alfan A, Syarif J, Atkinson HV. J Mater Sci 2011;46:7679.
[26] Bigot R, Becker E, Langlois L. Solid State Phenom 2013;192–193:521.
[27] Tzimas E, Zavaliangos A. J Mater Sci 2000;35:5319.